Ultrafast formation and decay dynamics of trions in *p*-doped single-walled carbon nanotubes

Takeshi Koyama,[1,*] Satoru Shimizu,[1] Yasumitsu Miyata,[2] Hisanori Shinohara,[2] and Arao Nakamura[1,†]
[1]*Department of Applied Physics, Graduate School of Engineering, Nagoya University, Chikusa, Nagoya 464-8603, Japan*
[2]*Department of Chemistry, Graduate School of Science, Nagoya University, Chikusa, Nagoya 464-8602, Japan*
(Received 28 November 2012; revised manuscript received 6 March 2013; published 19 April 2013)

We present the formation and decay dynamics of a trion (charged exciton) and exciton system in chemically *p*-doped single-walled carbon nanotubes (SWNTs) investigated by time-resolved photoluminescence measurements at 300 K. In (6,5) SWNTs with hole densities in the range of 0.27–1.05 nm^{-1}, a trion is formed from the coalescence of an exciton and a free hole, with a rate of 1.7×10^{13} nm s^{-1}. The linear dependence of the trion decay rate on the hole density allows us to find that the trion decay is governed by both a trion-hole Auger recombination process and an internal Auger recombination process. The observed high efficiencies of Auger processes dominate over the radiative recombination rate of trions, which demonstrates dynamic properties of excitonic complexes in the presence of enhanced Coulomb interactions in one-dimensional systems.

DOI: 10.1103/PhysRevB.87.165430 PACS number(s): 78.67.Ch, 78.47.jd, 78.55.−m

I. INTRODUCTION

A composite particle comprised of an exciton and an electron (or a hole) is known as a negative (positive) trion or a charged exciton, which is analogous to the charged hydrogen ions H^- and $H_2{}^+$. Since their first experimental observation in 1993,[1] trions have attracted considerable interest from both fundamental and technological viewpoints. Trions as well as excitons govern the optical properties of carrier-doped low-dimensional semiconductors,[2–4] and have potential applications in quantum-information science and related fields. In single-walled carbon nanotubes (SWNTs), recent studies have evidenced the stable formation of trions at room temperature because of their large binding energy.[5–8] Positive trions have been formed in chemically hole-doped (*p*-doped) SWNTs[6] and both negative and positive trions have been generated by an all-optical method[7] and an opto-electrochemical method.[8] However, the formation mechanism and localized or delocalized nature remain unknown, though Santos *et al.* suggested that electrons and holes are localized to avoid their spatial overlap and further recombination for all-optical trion generation.[7]

In $In_xGa_{1-x}As$ quantum wells (QWs), trions can be formed via a bimolecular process (an exciton and an electron/hole) or a trimolecular process (an unbound electron-hole pair and an electron/hole), depending on the excitation densities, and decay on a time scale of nanoseconds.[9] The formation time of trions is as long as ∼100 ps in modulation-doped GaAs/AlGaAs QWs[10] and 65 ps in *p*-doped CdTe/CdMgZnTe QWs,[11] reflecting the localized nature of trions resulting from potential fluctuations in the QWs. In SWNTs, scattering among excitons, charged excitons, and electrons (holes) is more significant because of enhanced Coulomb interactions in one-dimensional (1D) systems. While exciton-electron scattering is suppressed at low temperatures due to the cusp-like structure of the exciton dispersion, it drastically increases at room temperature.[12] Auger annihilation processes associated with enhanced Coulomb interactions between charged particles are expected to play a more important role in trion decay.

In this paper, we report the investigation of the dynamics of a trion and exciton system in *p*-doped SWNTs with hole densities of 0.27–1.05 nm^{-1} at room temperature by means of femtosecond time-resolved luminescence spectroscopy. The hole density dependence of the formation rate reveals that the trions are formed through a bimolecular process, i.e., the coalescence of an exciton and a free hole, with a rate of 1.7×10^{13} $nm^{-1}s^{-1}$. Trion decay is governed by both a trion-hole Auger recombination process with a rate of 1.0×10^{12} nm s^{-1} and an internal Auger recombination process with a rate of 1.4×10^{12} s^{-1}. We find that the internal Auger process, in which an electron-hole pair recombines with ejection of a hole within a trion, dominates over the radiative recombination process, which is the intrinsic nature of excitonic complexes in SWNTs.

II. EXPERIMENT

A. Sample preparation

The SWNTs used in this study were produced by the Co-Mo catalytic (CoMoCAT) process (SWeNT, SG-65). The nanotubes (25 mg quantity) were dispersed in water (50 ml) with 2% weight (wt) sodium dodecyl sulfate (SDS) by sonication at 15 °C for 5 h (Branson, Sonifier 450). The dispersion was immediately centrifuged at 122 000 g for 3 h (Hitachi Koki, 70P-72), and the upper 80% supernatant was then collected. The supernatant was used as the starting material for the gel column chromatography procedure[13,14] for enhancement of (6,5)-chirality SWNTs. A gel column was filled with 1 ml of Sephacryl S-200 (GE Healthcare) and then equilibrated by 2% wt SDS solution. 12 ml of the supernatant was poured into the gel column. 10 ml of 2% wt SDS solution was added into the column to wash out the unbound SWNTs. 4 ml of 5% wt SDS solution was added into the column to elute SWNTs bounded to the gel. The obtained dispersions were used as the samples. The majority of SWNTs were isolated, though there remained small bundles of several SWNTs.[15] The abundance ratios of SWNTs in the samples were estimated from the spectral weights of exciton absorptions. The abundance ratios of (6,5) and (6,4) SWNTs are enhanced from 59.7% to 74.1% and from 6.3% to 20.2% after the gel column chromatography procedure, respectively. Details of the characterization of samples are described in the Supplemental Material (see Ref. 16). Hole-doping of the

 ©2013 American Physical Society

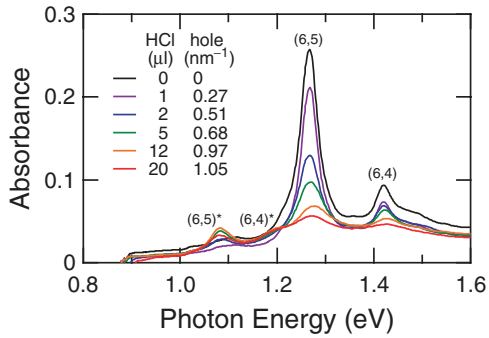

FIG. 1. (Color online) Absorption spectra of samples with addition of HCl solution. The amounts of HCl solution added for 600-μl SWNT dispersant and the estimated hole densities are indicated in the figure.

SWNTs was performed by adding an HCl solution[17,18] into the SWNT dispersion.

B. Experimental setup

Absorption spectra and maps of photoluminescence excitation (PLE) spectra were taken using a HITACHI U-3500 spectrophotometer and a Shimadzu CNT-RF system, respectively. Luminescence kinetics were measured using femtosecond time-resolved luminescence spectroscopy based on the frequency up-conversion technique.[19] The light source was a mode-locked Ti:sapphire laser operating at 82 MHz with a pulse width and wavelength of 80 fs and 800 nm, respectively (corresponding to a photon energy of 1.55 eV). The excitation intensity was $\sim$0.3 μJ cm^{-2}/pulse ($\sim$1 $\times$10^{12} photons cm^{-2}/pulse), which is well below the threshold ($\sim$50 μJ cm^{-2}/pulse) for the occurrence of the exciton-exciton annihilation process in (6,5) SWNTs under the 1.55-eV excitation condition.[20] We used a 0.3-mm-length cell to achieve a higher time resolution by diminishing a difference in propagation time within the sample between an excitation pulse and a luminescence signal, which is due to a difference in their group velocities. The instrument response function of the measurement system was determined by measuring a cross-correlation trace between the gate pulse and excitation pulse scattered from the sample surface, which had a Gaussian shape with a full width at half-maximum of 120 fs. In the fitting analysis, we used a convolution method, and the resolution of the fitted time constant was 20 fs. The spectral resolution was about 0.03 eV. All measurements were conducted at room temperature.

III. RESULTS AND DISCUSSION

A. Absorption and PLE spectra

Figure 1 shows the dependence of the absorption spectra of the samples on the amount of HCl solution added. The absorption bands observed in the undoped sample are attributed to the lowest singlet excitons (E_{11} excitons) of various SWNT species, and the major chiralities of (6,5) and (6,4) are assigned by referring to Ref. 21. The assignment of other SWNT species is shown in Fig. S1 in the Supplemental Material.[16] The spectral weights of the E_{11} exciton bands

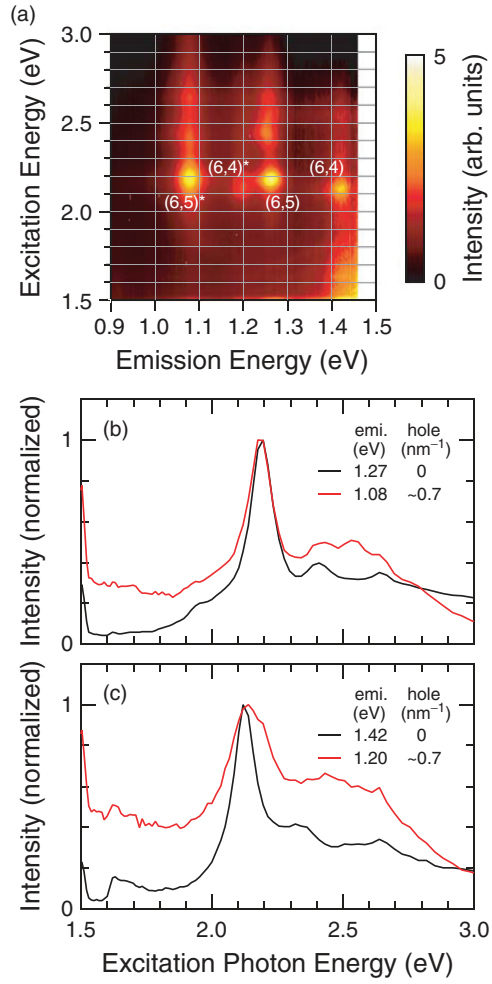

FIG. 2. (Color online) (a) PLE map of doped sample with a hole density of $\sim$0.7 nm^{-1}. (b) Excitation spectra for (6,5) SWNTs probed at 1.27 (undoped sample) and 1.08 eV (doped sample). (c) Excitation spectra for (6,4) SWNTs probed at 1.42 eV (undoped sample) and 1.20 eV (doped sample).

decrease with the addition of the HCl solution. According to Refs. 22 and 23, the ensemble average of hole density in the (6,5) SWNTs can be estimated by considering the band-filling effect of free holes that leads to a reduction in oscillator strength of the E_{11} exciton transition, and the estimated hole densities are indicated in the figure. As the hole density increases, two additional absorption bands appear at 1.08 and 1.20 eV [indicated as (6,5)* and (6,4)*], and their spectral weights increase. These bands are assigned to the trion absorption bands of (6,5) and (6,4) SWNTs by considering the energy differences from the E_{11} exciton bands;[6,7] this assignment is confirmed by PLE spectra, as discussed below.

A PLE map of the doped (hole density $\sim$0.7 nm^{-1}) sample is shown in Fig. 2(a). The fingerprints observed at the emission photon energies of 1.27 and 1.42 eV are attributed to the E_{11} excitons of the (6,5) and (6,4) SWNTs, as indicated in the figure. In addition to these fingerprints, two fingerprints are observed at emission photon energies of 1.08 and 1.20 eV [indicated as (6,5)* and (6,4)*] at which the two peaks are observed in the absorption spectra of the doped samples. The emission peaks can be assigned based on the excitation

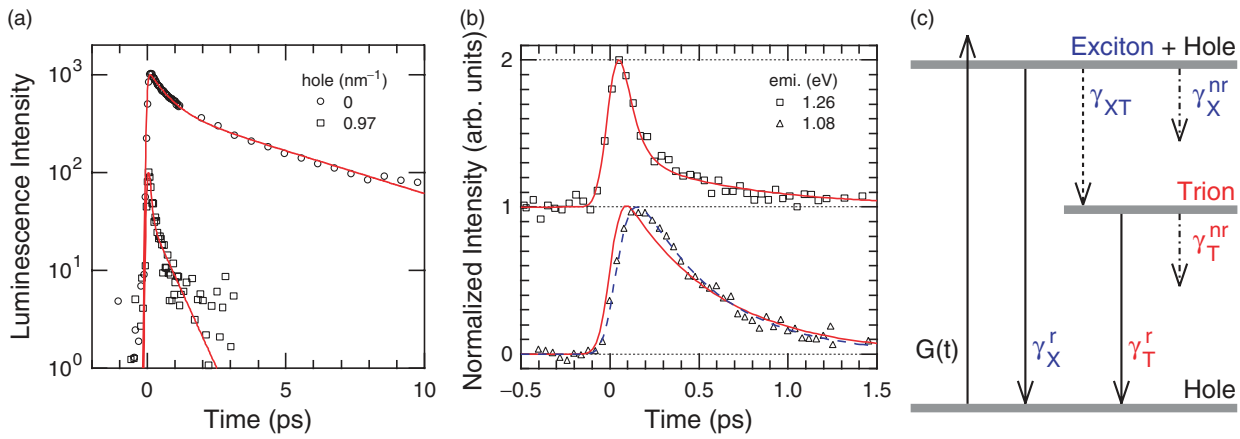

FIG. 3. (Color online) (a) Luminescence kinetics of E_{11} exciton at 1.26 eV in undoped (top) and doped (hole density 0.97 nm^{-1}) (bottom) samples. The symbols and solid curves represent experimental data and double-exponential fits, respectively. (b) Luminescence kinetics of trion at 1.08 eV (bottom) in doped sample (hole density 0.97 nm^{-1}) together with that of E_{11} exciton at 1.26 eV (top). The baselines are shifted for clarity. The symbols represent experimental data, and the solid and dashed curves are the results of double (single) exponential fits and of the fit using Eq. (2), respectively. (c) Schematic of relaxation processes of an exciton and trion in doped SWNTs.

spectra probed at 1.08 and 1.20 eV, shown in Figs. 2(b) and 2(c). The E_{11} exciton luminescence of the (6,5) SWNTs probed at 1.27 eV in the undoped sample is enhanced by the resonant excitation of the E_{22} exciton transition at 2.18 eV (black curve), and the luminescence probed at 1.08 eV in the doped sample is also enhanced at this energy (red curve). Therefore, this luminescence comes from (6,5) SWNTs. The difference between the E_{11} exciton luminescence energy and the hole-doping-induced luminescence energy is 0.19 eV in (6,5) SWNTs. As shown in Fig. 2(c), the excitation spectrum probed at 1.42 eV for (6,4) SWNTs in the undoped sample shows a peak at 2.13 eV that corresponds to the E_{22} exciton energy of the (6,4) SWNTs. The excitation spectrum probed at 1.20 eV in the doped sample shows the primary peak at the same energy (2.13 eV). The energy difference between the E_{11} luminescence energy (1.42 eV) and the hole-doping-induced luminescence energy (1.20 eV) in (6,4) SWNTs is 0.22 eV. These values are in good agreement with reported values for the energy difference between the singlet exciton state and the trion state: 0.18 eV in (6,5) SWNTs,[6] and 0.19 eV in (6,5) and 0.22 eV in (6,4) SWNTs.[7] Therefore, we attribute the bands observed at 1.08 and 1.20 eV in both the absorption and PLE spectra to trions in the (6,5) and (6,4) SWNTs, respectively. Hereafter, we focus on the results obtained for the (6,5) SWNTs (diameter of 0.75 nm), because the trion band is better separated from the exciton bands in the (6,5) SWNTs than in the (6,4) SWNTs.

B. Luminescence kinetics

Figure 3(a) shows the luminescence kinetics of the E_{11} exciton in (6,5) SWNTs at 1.26 eV in the undoped and doped (hole density 0.97 nm^{-1}) samples. As observed in our previous study,[24] the luminescence kinetics in the undoped sample shows fast and slow decay components, and can be fitted to a double-exponential function, $C\exp(-t/\tau_f) + (1-C)\exp(-t/\tau_s)$. Here, the time constants τ_f and τ_s are 640 ± 20 fs and 5.0 ± 0.2 ps, respectively, and the weighting factor C is 0.60 ± 0.05. Since the excitation density is $\sim 0.3\,\mu$J cm^{-2}/pulse and is well below the threshold of $\sim 50\ \mu$J cm^{-2}/pulse for the occurrence of the exciton-exciton annihilation process in (6,5) SWNTs,[20] the observed decay behavior reflects linear exciton decay dynamics. The fast and slow decay components respectively correspond to intertube exciton decay via excitation energy transfer in SWNT bundles remaining in the sample[19,25,26] and intratube exciton decay mainly due to nonradiative processes in isolated SWNTs.[27,28]

In the doped sample, the luminescence kinetics also shows biexponential decay behavior. However, the time constants in the doped sample are much shorter than in the undoped sample; τ_f and τ_s are 60 ± 20 and 540 ± 20 fs, respectively, and C is 0.80 ± 0.05. The shorter decay time of 60 fs in the doped sample indicates that an additional faster decay channel of the E_{11} exciton is induced by the hole doping. The phonon-assisted indirect exciton ionization (PAIEI) process[29] is the dominant decay channel in p-doped (8,6) SWNTs with hole densities below ~ 0.25 nm^{-1}.[23] The value of the exciton decay rate extrapolated to a hole density of ~ 1 nm^{-1} is 3.6×10^{11} s^{-1}, and is about two orders of magnitude smaller than the rate observed in our experiments [$1.7(\pm 0.6) \times 10^{13}$ s^{-1} = $(60 \pm 20$ fs$)^{-1}$]. Therefore, the fast decay component (major component) cannot be explained by the PAIEI process, suggesting the existence of other decay channels. The slow decay time of 540 fs is approximately the same as the fast decay time observed in the undoped sample. Therefore, the 540 fs decay component (minor component) in the doped sample is attributed to bundled SWNTs that are not thoroughly doped, probably because the dopants do not come into contact with the SWNTs within a bundle.

The luminescence kinetics of trions in (6,5) SWNTs are shown in Fig. 3(b) at 1.08 eV (bottom) in the doped sample with a hole density of 0.97 nm^{-1} together with that of the E_{11} exciton in (6,5) SWNTs at 1.26 eV (top).[30] In contrast to the decay kinetics of the E_{11} exciton luminescence at 1.26 eV, the decay curve of the trion luminescence at 1.08 eV shows exponential-like behavior. However, a simple single-exponential function with a time constant of 520 fs

cannot reproduce the observed behavior around the time origin, suggesting the existence of a rise component.

C. Rate equation analysis

To analyze the dynamical behavior of the luminescence from the (6,5) SWNTs using a rate equation model, we consider relaxation processes in the doped SWNTs, as shown schematically in Fig. 3(c). The E_{11} exciton consists of bright- and dark-exciton states. However, we neglect the dark-exciton state in the model, because the relaxation time of bright excitons to the dark-exciton state in undoped SWNTs is on the order of 10–100 ps[31,32] and much longer than the exciton decay times (60 and 540 fs) observed in our study.

Laser pulse excitation creates E_{11} excitons with a density of $N_X(t)$ by the generation function $G(t)$. Because of the large separation between the excitation photon energy of 1.55 eV and the trion state energy of 1.08 eV, the trion absorption is very weak at 1.55 eV, and thus we assume that the trion state is not directly excited by the laser pulse. The E_{11} excitons decay via radiative and nonradiative processes. The radiative decay rate is denoted by γ_X^r, and the nonradiative exciton decay processes include a decay to the trion state γ_{XT} and a decay to nonradiative centers γ_X^{nr}. Trion formation is expressed by the term $\gamma_{XT}N_X(t)$. The trions also decay via radiative (γ_T^r) and nonradiative (γ_T^{nr}) processes. Therefore, the rate equations for the exciton and trion densities $N_X(t)$ and $N_T(t)$ are written in the form

$$\frac{dN_X(t)}{dt} = G(t) - \left(\gamma_X^r + \gamma_X^{nr} + \gamma_{XT}\right)N_X(t), \qquad (1)$$

$$\frac{dN_T(t)}{dt} = \gamma_{XT}N_X(t) - \left(\gamma_T^r + \gamma_T^{nr}\right)N_T(t). \qquad (2)$$

The exciton decay rate in isolated undoped SWNTs is $\sim 10^{11}$ s^{-1},[27,28] and the decay rate due to the PAIEI process by hole doping is estimated to be 3.6×10^{11} s^{-1} for a hole density of ~ 1 nm^{-1}. Hence, $\gamma_X^r + \gamma_X^{nr}$ is fixed at 4.6×10^{11} s^{-1}, and we fit the trion decay curve by adjusting the parameters γ_{XT} and $(\gamma_T^r + \gamma_T^{nr})$. The fitted result is shown in Fig. 3(b) as a dashed line, and the obtained values of γ_{XT} and $(\gamma_T^r + \gamma_T^{nr})$ are $1.7(\pm 0.6) \times 10^{13}$ s^{-1} and $2.3(\pm 0.1) \times 10^{12}$ s^{-1}, respectively. The inverse of γ_{XT}, i.e., the trion rise time, is 60 ± 20 fs, in fairly good agreement with the decay time of 60 ± 20 fs for the E_{11} exciton luminescence shown in Fig. 3(a) indicating that the excitons decay to trions in 60 ± 20 fs.

Figure 4 shows luminescence decay curves of trions measured at 1.08 eV in (6,5) SWNTs with hole densities of 0.68, 0.97, and 1.05 nm^{-1}. They show the rise and single-exponential decay behavior. The observed curves are fitted well to the function in Eq. (2) and the results are plotted as dashed lines. The rise time, i.e., the inverse of γ_{XT}, decreases with increasing hole density: 80 ± 20 fs at 0.68 nm^{-1}, 60 ± 20 fs at 0.97 nm^{-1}, and 50 ± 20 fs at 1.05 nm^{-1}. The decay time of the trion luminescence also decreases with increasing hole density: 470 ± 20 at 0.68 nm^{-1}, 440 ± 20 fs at 0.97 nm^{-1}, and 400 ± 20 fs at 1.05 nm^{-1}.

D. Mechanisms of trion formation and decay processes

Shown in Fig. 5(a) is the γ_{XT} value obtained by fitting analysis as a function of the hole density n_p. We observe a linear dependence of γ_{XT} on n_p, and the extrapolated value of γ_{XT} is approximately zero at $n_p = 0$. This result indicates that trions are formed through an exciton-hole interaction, i.e., a bimolecular process. As shown in Fig. 3(b), no rise behavior of the exciton luminescence is observed, which indicates that the free electron-hole pairs instantaneously form excitons within the laser pulse duration. As a result, the trimolecular reaction is ineffective at forming trions. The high formation rate via the bimolecular reaction is consistent with recent theoretical calculations of exciton-electron scattering in doped SWNTs.[12] Exciton-electron elastic scattering is suppressed at the low temperature (Fig. 2 in Ref. 12) because of the cusp-like structure of the exciton dispersion, which is characteristic of semiconducting SWNTs. At the high temperature, however,

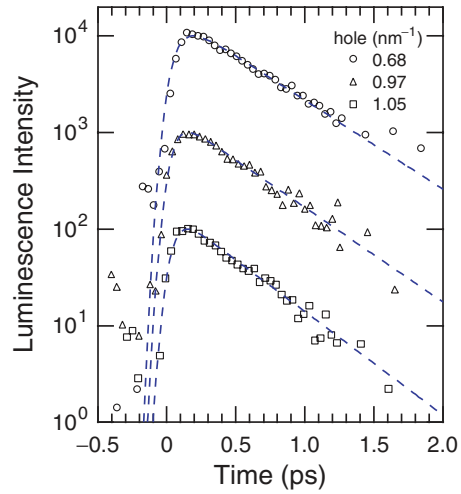

FIG. 4. (Color online) Luminescence kinetics of trions measured at 1.08 eV in (6,5) SWNTs with hole densities of 0.68, 0.97, and 1.05 nm^{-1}. The symbols represent experimental data. The dashed curves are the results of curve fitting using Eq. (2).

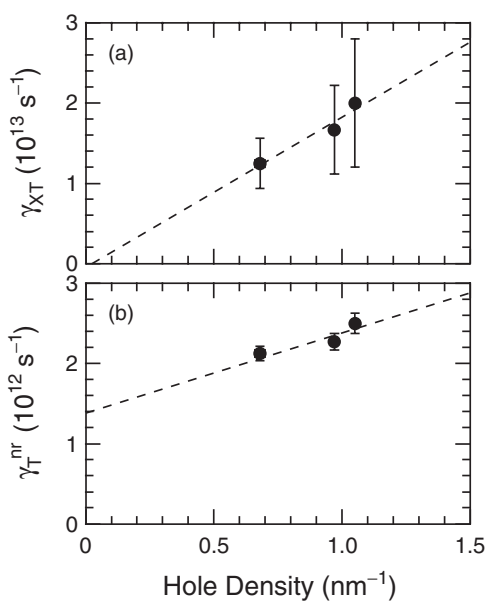

FIG. 5. Hole-density dependence of the (a) exciton-trion decay rate γ_{XT} and (b) nonradiative decay rate of trion γ_T^{nr}.

the scattering rate becomes high because the energy of the incoming electrons lies in the region of parabolic dispersion of the exciton. The scattering rate at 300 K for SWNTs with a diameter of 1 nm is estimated to be $\sim 3 \times 10^{13}$ s^{-1} for $n_p \sim 1$ nm^{-1} based on Fig. 5 and Eq. (3) from Ref. 12. The trion formation rate must be smaller than this value, since the phonon emission process is involved in the formation of a trion in the lowest state.

We now discuss the trion decay processes described by the rate of $(\gamma_T^r + \gamma_T^{nr})$. The radiative decay rate for trions is not known, but is expected to be lower than that for excitons, which is 10^8–10^9 s^{-1},[33,34] because of the mixed character of singlet and triplet states. As the observed decay rate of trions in our study is 2.1×10^{12}–2.5×10^{12} s^{-1}, nonradiative processes are dominant. As shown in Fig. 5(b), γ_T^{nr} increases linearly with n_p, which indicates trion-hole Auger recombination. As the transition energy of the trion (1.08 eV) almost equals the energy separation between the tops of the first and third valence bands of (6,5) SWNTs,[35] a hole in the vicinity of the top of the first valence band can be excited to the third valence band when an electron-hole pair within a trion recombines. Since the densities of states for the initial and final hole states are high near the van Hove singularities, such an Auger process takes place efficiently. Defining the rate as $\gamma_T^{nr} = An_p + B$, line fitting analysis yields the values of A and B to be 1.0×10^{12} nm s^{-1} and 1.4×10^{12} s^{-1}, respectively. The finite rate at $n_p = 0$ suggests the occurrence of an internal Auger recombination process in which an electron-hole pair recombines, with ejection of a hole within a trion. For $n_p = 1$ nm^{-1}, the trion-hole Auger rate is 1.0×10^{12} s^{-1}, comparable to the internal Auger rate. Since the size of the trion wave function is $\sim$5 nm,[5,36] the effective distance between an electron and hole (or holes) is on the same order of magnitude as ${n_p}^{-1}$ for high hole densities. Therefore, it is reasonable that the rate of the trion-hole Auger process, wherein a hole not forming a trion is scattered, is comparable to that of the internal Auger process, wherein a hole forming a trion is scattered.

We note that the internal Auger rate is higher than the exciton annihilation rate by the PAIEI process in which an exciton annihilates via scattering with a hole with emission of phonons; the PAIEI rate is estimated to be 3.6×10^{11} s^{-1} for $n_p = 1$ nm^{-1}. Although an electron and two holes are involved in both recombination processes, the Auger rate is higher when the three particles form an excitonic complex by the Coulomb interaction. Very recently, Colombier *et al.*[37] reported that a biexciton does exist in SWNTs and becomes annihilated through the Auger process with a rate of 2×10^{12} s^{-1}, which is comparable to the exciton-exciton annihilation and the Auger processes of the trion. Therefore, these results indicate that high efficiencies of Auger processes are inherent in excitonic complexes in SWNTs. A theoretical study of trion-hole (electron) interactions and a role of phonon is needed for a detailed understanding of Auger processes.

IV. CONCLUSION

We have investigated the dynamic properties of excitons and trions in p-doped semiconducting SWNTs with hole densities of 0.27–1.05 nm^{-1} at room temperature. Time-resolved luminescence measurements of (6,5) SWNTs allowed us to determine that the trion is formed from an exciton and a free hole with a formation rate of 1.7×10^{13} nm s^{-1}. The decay rate of trions shows a linear dependence on the hole density, which indicates that the trion decay is governed by both a trion-hole Auger recombination process and an internal Auger recombination process, dominating over the radiative process. The internal Auger recombination rate is 1.4×10^{12} s^{-1} and the trion-hole Auger recombination rate is 1.0×10^{12} s^{-1} for $n_p = 1$ nm^{-1}. The observed high Auger rates dominate over the radiative recombination rate of trions. Our findings provide further insights into recombination processes of excitonic complexes in the presence of enhanced Coulomb interactions in 1D systems and stimulates further theoretical work for such systems.

ACKNOWLEDGMENTS

This work was supported by KAKENHI from JSPS (Grant No. 21340081) and MEXT of Japan (Grant No. 22016004).

*Correspondence should be addressed to koyama@nuap.nagoya-u.ac.jp

†Present address: Toyota Physical and Chemical Research Institute, Nagakute, Aichi 480-1192, Japan.

[1] K. Kheng, R. T. Cox, Y. Merle d'Aubigné, F. Bassani, K. Saminadayar, and S. Tatarenko, Phys. Rev. Lett. **71**, 1752 (1993).

[2] G. Finkelstein, H. Shtrikman, and I. Bar-Joseph, Phys. Rev. Lett. **74**, 976 (1995).

[3] R. J. Warburton, C. S. Dürr, K. Karrai, J. P. Kotthaus, G. Medeiros-Ribeiro, and P. M. Petroff, Phys. Rev. Lett. **79**, 5282 (1997).

[4] H. Akiyama, L. N. Pfeiffer, A. Pinczuk, K. W. West, and M. Yoshita, Solid State Commun. **122**, 169 (2002).

[5] T. F. Rønnow, T. G. Pedersen, and H. D. Cornean, Phys. Rev. B **81**, 205446 (2010); J. Phys. A **43**, 474031 (2010).

[6] R. Matsunaga, K. Matsuda, and Y. Kanemitsu, Phys. Rev. Lett. **106**, 037404 (2011).

[7] S. M. Santos, B. Yuma, S. Berciaud, J. Shaver, M. Gallart, P. Gilliot, L. Cognet, and B. Lounis, Phys. Rev. Lett. **107**, 187401 (2011).

[8] J. S. Park, Y. Hirana, S. Mouri, Y. Miyauchi, N. Nakashima, and K. Matsuda, J. Am. Chem. Soc. **134**, 14461 (2012).

[9] M. T. Portella-Oberli, J. Berney, L. Kappei, F. Morier-Genoud, J. Szczytko, and B. Deveaud-Plédran, Phys. Rev. Lett. **102**, 096402 (2009).

[10] G. Finkelstein, V. Umansky, I. Bar-Joseph, V. Ciulin, S. Haacke, J.-D. Ganière, and B. Deveaud, Phys. Rev. B **58**, 12637 (1998).

[11] E. Vanelle, M. Paillard, X. Marie, T. Amand, P. Gilliot, D. Brinkmann, R. Lévy, J. Cibert, and S. Tatarenko, Phys. Rev. B **62**, 2696 (2000).

[12] S. Konabe, K. Matsuda, and S. Okada, Phys. Rev. Lett. **109**, 187403 (2012).

[13] H. Liu, D. Nishide, T. Tanaka, and H. Kataura, Nat. Commun. **2**, 309 (2011).

[14]Y. Miyata, K. Shiozawa, Y. Asada, Y. Ohno, R. Kitaura, T. Mizutani, and H. Shinohara, Nano Res. **4**, 963 (2011).

[15]J. Crochet, M. Clemens, and T. Hertel, J. Am. Chem. Soc. **129**, 8058 (2007).

[16]See Supplemental Material at http://link.aps.org/supplemental/10.1103/PhysRevB.87.165430 for details of the characterization of samples.

[17]M. S. Strano, C. B. Huffman, V. C. Moore, M. J. O'Connell, E. H. Haroz, J. Hubbard, M. Miller, K. Rialon, C. Kittrell, S. Ramesh, R. H. Hauge, and R. E. Smalley, J. Phys. Chem. B **107**, 6979 (2003).

[18]G. N. Ostojic, S. Zaric, J. Kono, M. S. Strano, V. C. Moore, R. H. Hauge, and R. E. Smalley, Phys. Rev. Lett. **92**, 117402 (2004).

[19]T. Koyama, Y. Miyata, K. Asaka, H. Shinohara, Y. Saito, and A. Nakamura, Phys. Chem. Chem. Phys. **14**, 1070 (2012).

[20]A. Ueda, K. Matsuda, T. Tayagaki, and Y. Kanemitsu, Appl. Phys. Lett. **92**, 233105 (2008).

[21]R. B. Weisman and S. M. Bachilo, Nano Lett. **3**, 1235 (2003).

[22]G. Dukovic, B. E. White, Z. Zhou, F. Wang, S. Jockusch, M. L. Steigerwald, T. F. Heinz, R. A. Friesner, N. J. Turro, and L. E. Brus, J. Am. Chem. Soc. **126**, 15269 (2004).

[23]K. Matsuda, Y. Miyauchi, T. Sakashita, and Y. Kanemitsu, Phys. Rev. B **81**, 033409 (2010).

[24]T. Koyama, S. Shimizu, T. Saito, Y. Miyata, H. Shinohara, and A. Nakamura, Phys. Rev. B **85**, 045428 (2012).

[25]I. V. Rubtsov, R. M. Russo, T. Albers, P. Deria, D. E. Luzzi, and M. J. Therien, Appl. Phys. A **79**, 1747 (2004).

[26]T. Koyama, Y. Miyata, Y. Asada, H. Shinohara, H. Kataura, and A. Nakamura, J. Phys. Chem. Lett. **1**, 3243 (2010); T. Koyama, K. Asaka, N. Hikosaka, H. Kishida, Y. Saito, and A. Nakamura, *ibid.* **2**, 127 (2011).

[27]S. Reich, M. Dworzak, A. Hoffmann, C. Thomsen, and M. S. Strano, Phys. Rev. B **71**, 033402 (2005).

[28]A. Hagen, M. Steiner, M. B. Raschke, C. Lienau, T. Hertel, H. Qian, A. J. Meixner, and A. Hartschuh, Phys. Rev. Lett. **95**, 197401 (2005).

[29]V. Perebeinos and Ph. Avouris, Phys. Rev. Lett. **101**, 057401 (2008).

[30]We confirmed that the contribution of the E_{11} exciton luminescence due to other SWNT species is negligibly small, and the trion luminescence of (6,5) SWNTs is the exclusive component; for details, see Fig. S2 in the Supplemental Material (Ref. 16).

[31]S. Berciaud, L. Cognet, and B. Lounis, Phys. Rev. Lett. **101**, 077402 (2008).

[32]R. Matsunaga, Y. Miyauchi, K. Matsuda, and Y. Kanemitsu, Phys. Rev. B **80**, 115436 (2009).

[33]C. D. Spataru, S. Ismail-Beigi, R. B. Capaz, and S. G. Louie, Phys. Rev. Lett. **95**, 247402 (2005).

[34]V. Perebeinos, J. Tersoff, and Ph. Avouris, Nano Lett. **5**, 2495 (2005).

[35]See Fig. S1(b) in the Supplemental Material[16] for details of transition energies of E_{22} and E_{33} excitons.

[36]K. Watanabe and K. Asano, Phys. Rev. B **85**, 035416 (2012).

[37]L. Colombier, J. Selles, E. Rousseau, J. S. Lauret, F. Vialla, C. Voisin, and G. Cassabois, Phys. Rev. Lett. **109**, 197402 (2012).